Mg-Zn-{Y, Ce} Alloys: Thermodynamic Modeling and Mechanical Properties

Subjects: Metallurgy & Metallurgical Engineering
Contributor: Mohammad Aljarrah

Magnesium alloys are a strong candidate for various applications in automobile and aerospace industries due to their low density and specific strength. Micro-alloying magnesium with zinc, yttrium, and cerium enhances mechanical properties of magnesium through grain refinement and precipitation hardening.

Keywords: thermodynamic modeling ; magnesium ; phase diagram ; liquidus projection

1. Introduction

Micro-alloying magnesium with RE such as zinc and yttrium resulted in promising mechanical properties [1][2][3][4][5][6][7][8][9]. Furthermore, the addition of RE elements to Mg-Zn promote activation of prismatic slip and increase the stacking fault energy, therefore weakening the texture of magnesium alloys [3][10][11][12][13][4][5][14][15][16][17]. Micro-alloying magnesium with zinc increases its fluidity in casting [18], whereas yttrium addition has a remarkable effect on aging precipitation and high solid solution strengthening [19][20][21]. Moreover, cerium tends to precipitate a thermally high stable compound (Mg_2Ce) in magnesium rich region, which improve microstructure stability at elevated temperatures. Diluting zinc in Mg-Ce alloy significantly improves stretch formability by modifying the basal plane texture through solid solution hardening mechanism [22][23][24][25][26]. Moreover, the highest zinc in Mg-Ce alloy improves yield strength and ultimate tensile strength through precipitation of intermetallic compounds. Whereas the ratio of Ce/Zn increases, grain refinements and loss of formability occurs [27][22][23][24][25][26][28][29][30]. Mg-Zn-Y alloys display promising mechanical properties because of precipitates of thermally stable ternary compounds (W-Mg_3Y solid solution, I-Mg_3YZn_6, and LPSO-phase $Mg_{12}ZnY$) as well as high solubility of yttrium in magnesium.

To better understand phase stability, phase relation, and the effect of precipitation on age hardening, knowledge of binary and ternary phase diagrams is essential. Additionally, accurate prediction of phase diagram plays an important role in materials development and alloy design. Phase diagram is a tool used to predict the equilibrium phase(s) and phase(s) percentage at certain temperatures for specified alloys and simulate the phase consistency and solidification process of individual alloys. Moreover, the percentage of the predicted phase(s) that exist in the microstructure can be calculated.

2. Zinc-Yttrium Phase Diagram

In the work of [31][32], tantalum containers were unsuccessful because of the penetration of Y-Zn liquid at high zinc contents. Mason and Chiotti [32] reported three intermetallic compounds that melt congruently: YZn, YZn_2, and Y_2Zn_{17} ($YZn_{8.5}$) at 1105, 1080, and 890 °C, respectively. Thermodynamic modeling of Y-Zn binary phase diagram in the work of [33][34][35] presented a polymorphic transformation in the YZn_2 at 750 °C, which is in accord with [32][36]. Mason and Chiotti [32] found five intermetallic compounds that decompose peritectically: YZn_3, Y_3Zn_{11} ($YZn_{3.67}$), $Y_{13}Zn_{58}$ ($YZn_{4.46}$), YZn_6, and YZn_{12} at 905, 896, 882, 872, and 685 °C, respectively. Mason and Chiotti [32] determined the thermodynamic properties of the intermetallic compounds using dewpoint method. The large number of intermetallic compounds found in the RE-Zn system was similar and related to RE-coordination number [37]. Crystal structure data of Y-Zn compounds were determined by [37][38][39][40]. Gibbs energy of formation of the intermediate compounds in the Y-Zn system was investigated by [41][42][43][44][45]. The most accurate description of Y-Zn binary phase diagram was established by Zhu and Pelton [46] based on experimental data [31][32] as shown in **Figure 1** and **Figure 2**. The optimized Y-Zn phase diagram presented by Zhu and Pelton [46] presented some amendment to the work of Spencer et al. [35]. The calculated enthalpy and Gibbs energies of formation of the intermetallic compound presented in the work of [35] are in good agreement with the experimental data of [32][41][42][45].

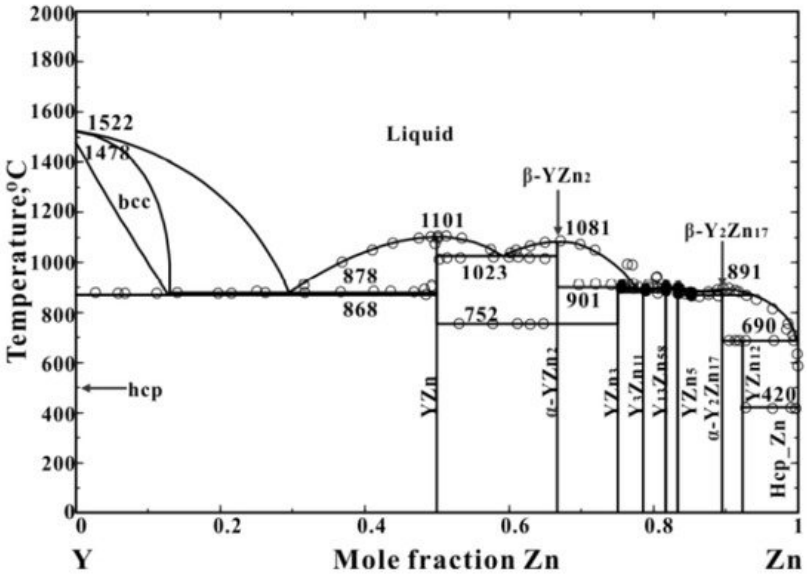

Figure 1. Yttrium–zinc phase diagram [46].

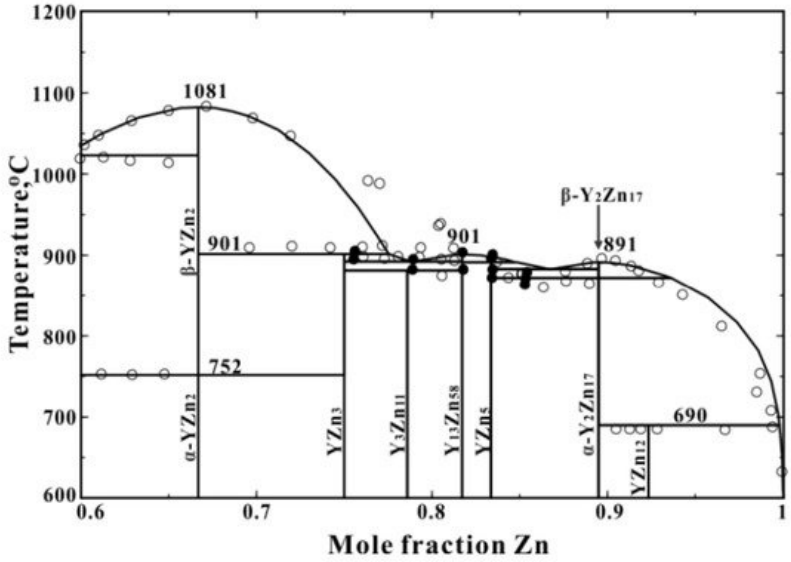

Figure 2. Yttrium–zinc phase diagram in Zn-rich region [46].

3. Mg-Zn, Mg-Y, and Mg-Ce Phase Diagrams

Liquid phase in the work of [18] was optimized using the modified quasi-chemical model (MQM). This model has been used to describe the liquid phase as this is the only scientific model that accounts for the presence of short-range ordering. Therefore, the reported phase diagrams in the work of [18] adequately describe thermodynamic properties of these systems. Islam et al. [18] critically reviewed and assessed thermodynamic data and phase diagrams of Mg-Zn, Mg-Y, and Mg-Ce systems. **Figure 3**, **Figure 4** and **Figure 5** presented the most accurate calculated binary phase diagrams for these systems [18]. It is worth mentioning that the liquid phase was optimized using a modified quasi-chemical model to accurately describe short range ordering in the liquid.

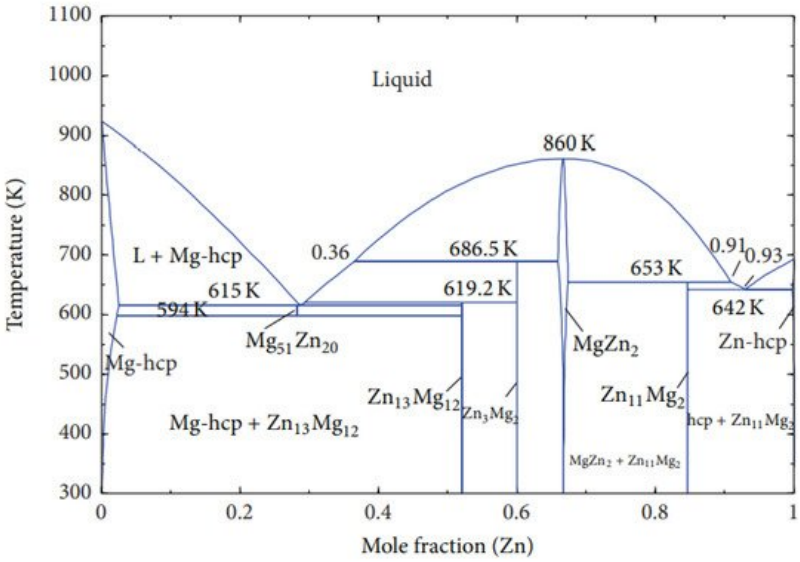

Figure 3. Mg-Zn phase diagram [47].

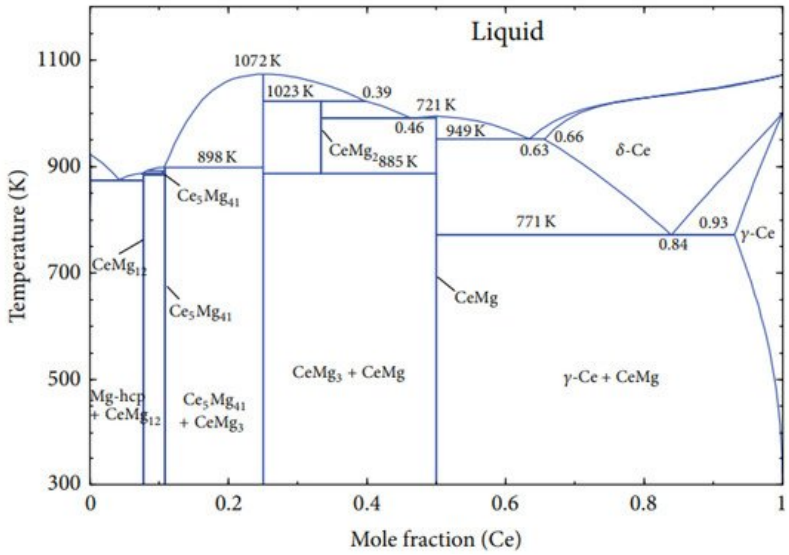

Figure 4. Mg-Ce phase diagram [18].

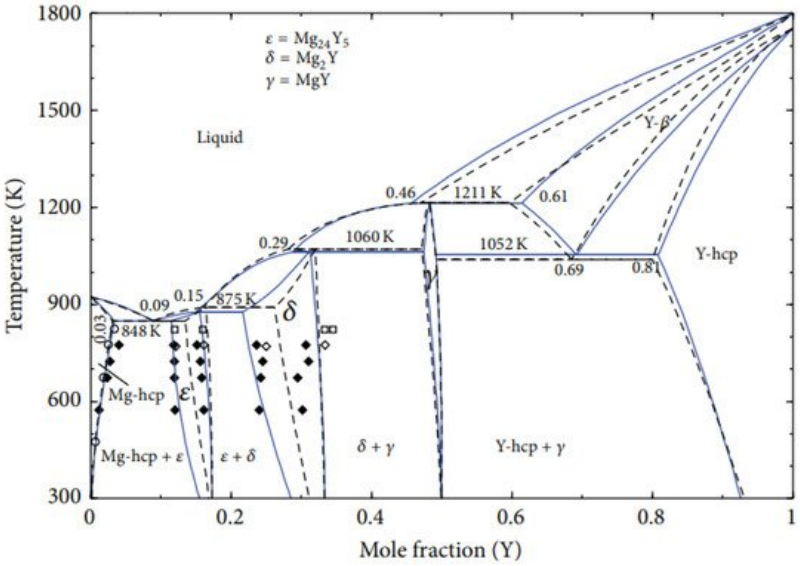

Figure 5. Mg-Y phase diagram solid lines [34] in comparison to [48] showed in dotted line [18].

4. Magnesium-Zinc-Yttrium Ternary Phase Diagram

Liquidus projections of the ternary Mg-Zn-Y phase diagram reported by Gröbner et al. [49] and Zhu and Pelton [50] are shown in **Figure 6**a,b, respectively.

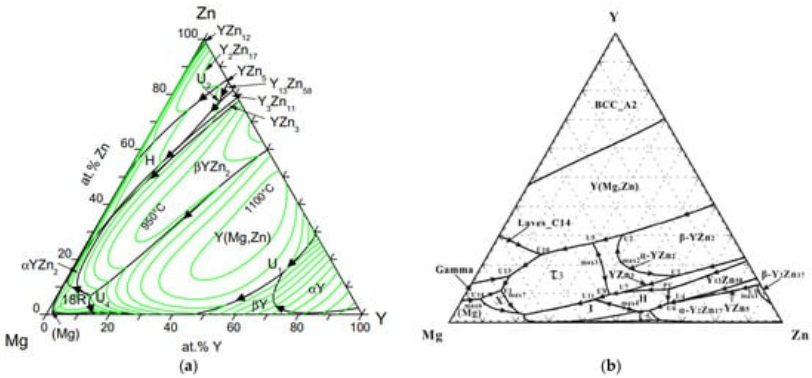

Figure 6. Liquidus projections of the ternary Mg-Zn-Y phase diagram; (**a**) Gröbner et al. [49] and (**b**) Zhu and Pelton [50].

5. Mechanical Properties of Mg-Zn-{Ce, Y} Alloys

Alloying Mg-Zn with rare earth elements is promising in modifying magnesium texture. Among rare-earth element, many researchers reported that micro-alloying Mg-Zn with yttrium or cerium exhibited a comparable ductility and formability with commercial magnesium alloys. **Table 1** and **Table 2** summarize the mechanical properties of the published alloys in Mg-Zn-Y [51][52][53][54] and Mg-Zn-Ce [55][27][22][26][53][54][56], respectively.

Table 1. Mechanical properties of Mg-Zn-Y alloys.

Nominal Composition (wt.%)	Yield Strength (MPa)	Ultimate Tensile Strength (MPa)	Ductility	Process Conditions
Mg-2Zn+0.4Y	160	240	30%	Samples were cast at 690 °C and then extruded at 310 °C [51]
Mg-14.4Zn-3.3Y	365 ± 3.5	380	8%	Samples were cast and solutionized at 480 °C for 24 h followed by extrusion at 430 °C, then aged at 150 °C [52]
Mg-14.4Zn-3.3Y	171	320	12	Samples were cast and solutionized at 480 °C for 24 h followed by extrusion at 430 °C [52]
Mg-1.5Zn-0.2Y	135	238	17%	The ingots were homogenized at 450 °C for 12 h, then rolled at 400 °C, and after that sheet annealed at 350 °C for 1 h [53]
Mg-6.0Zn-1.0Y	268.3		12.9%	Alloys were solutionized at 480 °C and then extruded at 390 °C [54]
Mg-6.0Zn-1.0Y	288.7		17.3%	Alloys were solutionized at 480 °C and then extruded at 390 °C and aged at 150 °C for 48h [54]
Mg-3.0Zn-0.5Y	262	18.3%		Alloys were solutionized at 480 °C and then extruded at 350 °C [54]

Table 2. Mechanical properties of Mg-Zn-Ce alloys.

Nominal Composition (wt.%)	Yield Strength (MPa)	Ultimate Tensile Strength (MPa)	Ductility	Process Conditions
Mg-2Zn+0.4Ce	190	255	18%	Samples were cast at 690 °C and then extruded at 310 °C [55]
Mg-2Zn-0.2Ce (ZE20)	69	170	31%	
Mg-5Zn-0.2Ce (ZE50)	135	247	15%	Samples were cast at 700 °C and then extruded at 400 °C [55]
Mg-8Zn-0.2Ce (ZE80)	136	289	16%	
Mg-1.5Zn-0.2Ce	140	240	19%	The ingots were homogenized at 450 °C for 12h, then rolled at 400 °C and after that sheet annealed at 350° C for 1 h [53]
Mg-6Zn-0.2Ce	225	270	30%	Alloys were cast at 750 °C and homogenized at 350 °C for 12 h. After extrusion, alloys aged at 175 °C from 0.5 to 80 h [54]

Nominal Composition (wt.%)	Yield Strength (MPa)	Ultimate Tensile Strength (MPa)	Ductility	Process Conditions
Mg-2%Zn-0.5%Ce (ZE20)	199.2	~245	6%	Samples were prepared by continuous casting, then homogenized at 823 K for 8 h. Sheets were rolled by conventional rolling at 673 K [56]
Mg-2%Zn-0.5%Ce (ZE20)	125	~235	13.8%	Samples were prepared by continuous casting, then homogenized at 823 K for 8 h. Sheets were rolled by conventional rolling at 673 K. Sheets were annealed at 673 K [56]
Mg-2%Zn-0.5%Ce (ZE20)	~170	~240	28.23	Samples were prepared by continuous casting, then homogenized at 823 K for 8 h. Sheets were rolled by packed rolling at 673 K. Sheets were annealed at 673 K [56]
Mg-2%Zn-0.5%Ce (ZE20)	~165	~236	33.4%	Samples were prepared by continuous casting, then homogenized at 823 K for 8 h. Sheets were rolled by packed rolling at 723 K. Sheets were annealed at 723 K [56]
Mg-0.5Zn-0.2Ce	133	213	25%	Samples were heated at 723 K for 20 min and sheets were rolled by unidirectional rolling at 353 K. Then, sheets were annealed at 623 K for 90 min [22]
Mg-1.0Zn-0.2Ce	110	202	23%	
Mg-1.5Zn-0.2Ce	116	206	29%	
Mg-2.0Zn-0.2Ce	118	222	25%	
Mg-2.5Zn-0.2Ce	131	228	16%	
Mg-1.5Zn-0.2Ce	153	231	26%	Samples were extruded at 703 K and then annealed at 623K for 90 min [26]
Mg-1.5Zn-0.2Ce	194	248	20%	Samples were extruded at 573K and then annealed at 623K for 90 min [26]
Mg-1.0Zn-1.0Ce	95	191	22%	Samples were annealed at 350 °C and then annealed at 450 °C for 1 h [27]
Mg-2.0Zn-1.0Ce	101	197	26.2%	
Mg-4Zn-1.0Ce	109	220	18%	
Mg-1.0Zn-0.5Ce	95	191	30%	

The addition of yttrium to Mg-Zn alloys enhances the formation of magnesium solid solution in ternary systems due to high solid solubility of yttrium in magnesium. Meanwhile, precipitation of nano-scale ternary phases as a result enhances mechanical properties.

References

1. Pérez, P.; Cabeza, S.; Garcés, G.; Adeva, P. Influence of long period stacking ordered phase arrangements on the corr osion behaviour of extruded Mg97Y2Zn1 alloy. Corros. Sci. 2016, 107, 107–112.
2. Chen, B.; Lin, D.; Zeng, X.; Lu, C. Effects of yttrium and zinc addition on the microstructure and mechanical properties of Mg–Y–Zn alloys. J. Mater. Sci. 2010, 45, 2510–2517.
3. Tong, L.B.; Li, X.H.; Zhang, H.J. Effect of long period stacking ordered phase on the microstructure, texture, and mecha nical properties of extruded Mg–Y–Zn alloy. Mater. Sci. Eng. A 2013, 563, 177–183.
4. Kawamura, Y.; Yamasaki, M. Formation and mechanical properties of Mg97Zn1RE2 alloys with long-period stacking or dered structure. Mater. Trans. 2007, 48, 2986–2992.
5. Yamasaki, M.; Hashimoto, K.; Hagihara, K.; Kawamura, Y. Effect of multimodal microstructure evolution on mechanical properties of Mg–Zn–Y extruded alloy. Acta Mater. 2011, 59, 3646–3658.
6. Li, B.; Hou, X.; Teng, B. Effects of friction stir process and subsequent aging treatment on the microstructure evolution and mechanical properties of Mg-Gd-Y-Zn-Zr alloy. Mater. Charact. 2019, 155, 109832.
7. Garces, G.; Muñoz-Morris, M.A.; Morris, D.G.; Perez, P.; Adeva, P. Optimization of strength by microstructural refineme nt of MgY2Zn1 alloy during extrusion and ECAP processing. Mater. Sci. Eng. A 2014, 614, 96–105.

8. Zhang, W.; Huo, W.T.; Lu, J.W.; Hu, J.J.; Wei, Q.; Zhang, Y.S. Gradient shear banding in a magnesium alloy induced by sliding friction treatment. Vacuum 2017, 143, 95–97.
9. Zhao, D.; Chen, X.; Wang, X.; Pan, F. Effect of impurity reduction on dynamic recrystallization, texture evolution and mechanical anisotropy of rolled AZ31 alloy. Mater. Sci. Eng. A 2020, 773, 138741.
10. Zhu, S.M.; Lapovok, R.; Nie, J.F.; Estrin, Y.; Mathaudhu, S.N. Microstructure and mechanical properties of LPSO phase dominant Mg 85.8 Y 7.1 Zn 7.1 and Mg 85.8 Y 7.1 Ni 7.1 alloys. Mater. Sci. Eng. A 2017, 692, 35–42.
11. Victoria-Hernández, J.; Yi, S.; Klaumünzer, D.; Letzig, D. Recrystallization behavior and its relationship with deformation mechanisms of a hot rolled Mg-Zn-Ca-Zr alloy. Mater. Sci. Eng. A 2019, 761, 138054.
12. Zhang, W.; Wei, Q.; Huo, W.T.; Lu, J.W.; Hu, J.J.; Zhang, Y.S. Dynamic recrystallization in nanocrystalline AZ31 Mg-alloy. Vacuum 2017, 143, 236–240.
13. Xu, D.; Han, E.; Xu, Y. Effect of long-period stacking ordered phase on microstructure, mechanical property, and corrosion resistance of Mg alloys: A review. Proc. Natl. Sci.-Mater. 2016, 26, 117–128.
14. Zhang, W.; Lu, J.; Huo, W.; Zhang, Y.; Wei, Q. Microstructural evolution of AZ31 magnesium alloy subjected to sliding friction treatment. Philos. Mag. 2018, 98, 1576–1593.
15. Aljarrah, M.; Essadiqi, E. On the precipitates and mechanical properties of magnesium-yttrium sheets. Alex. Eng. J. 2013, 52, 221–225.
16. Wei, Y.H.; Liu, B.S.; Hou, L.F.; Xu, B.S.; Liu, G. Characterization and properties of nanocrystalline surface layer in Mg alloy induced by surface mechanical attrition treatment. J. Alloys Compd. 2008, 452, 336–342.
17. Aljarrah, M.; Essadiqi, E.; Fouad, R.H.; Rababah, M.; Almagableh, A. The effect of annealing conditions and alloying elements on the microstructure stability and mechanical properties of Mg-Zn-Ce sheets. Appl. Mech. Mater. 2014, 472, 937–947.
18. Wang, G.; Huang, G.; Chen, X.; Deng, Q.; Tang, A.; Jiang, B.; Pan, F. Effects of Zn addition on the mechanical properties and texture of extruded Mg-Zn-Ca-Ce magnesium alloy sheets. Mater. Sci. Eng. A 2017, 705, 46–54.
19. Islam, M.M.; Mostafa, A.O.; Medraj, M. Essential magnesium alloys binary phase diagrams and their thermodynamic data. J. Mater. 2014, 2014, 704283.
20. Stanford, N.; Cottam, R.; Davis, B.; Robson, J. Evaluating the Effect of Yttrium as a Solute Strengthener in Magnesium Using in Situ Neutron Diffraction. Acta Mater. 2014, 78, 1–13.
21. Gao, L.; Chen, R.S.; Han, E.H. Solid Solution Strengthening Behaviors in Binary Mg–Y Single Phase Alloys. J. Alloys Compd. 2009, 472, 234–240.
22. Gao, L.; Chen, R.S.; Han, E.H. Effects of Rare-Earth Elements Gd and Y on the Solid Solution Strengthening of Mg Alloys. J. Alloys Compd. 2009, 481, 379–384.
23. Chino, Y.; Huang, Z.; Suzuki, K.; Sassa, K.; Mabuchi, M. Influence of Zn concentration on stretch formability at room temperature of Mg-Zn-Ce alloy. Mater. Sci. Eng. A 2010, 528, 566–572.
24. Zhou, T.; Xia, H.; Chen, Z.H. Effect of Ce on microstructures and mechanical properties of rapidly solidified Mg–Zn alloy. Mater. Sci. Tech. 2011, 27, 1198–1205.
25. Langelier, B.; Esmaeili, S. Effects of Ce additions on the age hardening response of Mg–Zn alloys. Mater. Charact. 2015, 101, 1–8.
26. Luo, A.A.; Mishra, R.K.; Sachdev, A.K. High-ductility magnesium-zinc-cerium extrusion alloys. Scr. Mater. 2011, 64, 410–413.
27. Li, C.Q.; Xu, D.K.; Zeng, Z.R.; Wang, B.J.; Sheng, L.Y.; Chen, X.B.; Han, E.H. Effect of volume fraction of LPSO phases on corrosion and mechanical properties of Mg-Zn-Y alloys. Mater. Des. 2017, 121, 430–441.
28. Chino, Y.; Huang, X.; Suzuki1, K.; Sassa, K.; Mabuchi, M. Microstructure, Texture and Mechanical Properties of Mg-Zn-Ce Alloy Extruded at Different Temperatures. Mater. Trans. 2011, 52, 1104–1107.
29. Mackenzie, L.W.F.; Pekguleryuz, M.O. The recrystallization and texture of magnesium-zinc-cerium alloys. Scr. Mater. 2008, 59, 665–668.
30. Guo, X.; Remennik, S.; Xu, C.; Shechtman, D. Development of Mg-6.0%Zn-1.0%Y-0.6%Ce-0.6% Zr magnesium alloy and its microstructural evolution during processing. Mater. Sci. Eng. A 2008, 473, 266–273.
31. Chiotti, P.; Mason, J.T.; Gill, K.J. Phase Diagram and Thermodynamic Properties of the Yttrium—Zinc System. Trans. TMS-AIME 1963, 227, 910–916.
32. Mason, J.T.; Chiotti, P. Phase diagram and thermodynamic properties of the yttrium-zinc system. Metall. Trans. A 1976, 7, 287–291.

33. Shao, G.; Varsani, V.; Fan, Z. Thermodynamic modelling of the Y-Zn and Mg-Zn-Y systems. Calphad 2006, 30, 286–295, Erratum in Calphad 2007, 31, 313.
34. Liu, X.J.; Wen, M.Z.; Wang, C.P.; Pan, F.S. Thermodynamic assessment of the Zn-Y and Al-Zn-Y systems. J. Alloys Compd. 2008, 452, 283–290.
35. Spencer, P.J.; Pelton, A.D.; Kang, Y.B.; Chartrand, P.; Fuerst, C.D. Thermodynamic assessment of the Ca-Zn, Sr-Zn, Y-Zn and Ce-Zn systems. Calphad 2008, 32, 423–431.
36. Harsha, K.S. The Crystal Structures of Intermetallic Compounds in the Yttrium-Zinc System. Ph.D. Thesis, Pennsylvania State University, State College, PA, USA, 1964.
37. Veleckis, E.; Schablaske, R.V.; Johnson, I.; Feder, H.M. Intermetallic phases in the systems of zinc with lanthanum, cerium, praseodymium, neodymium, and yttrium. Trans. TMS-AIME 1967, 239, 58.
38. Bruzzone, G.; Fornasini, M.L.; Merlo, F. Rare-earth intermediate phases with zinc. J. Less-Common Met. 1970, 22, 253–264.
39. Fornasini, M.L. Crystal structnre of (Ho-, Er-, Tm-, Lu-, Y-) Zn, and ThCd5 intermetallic compounds. J. Less-Common Met. 1971, 25, 329–333.
40. Ryba, E. Transformation in AB2 Intermetallic Compounds, US Atomic Energy Comm. Report COO-3415-3. 1963. Available online: https://www.osti.gov/servlets/purl/4272069 (accessed on 7 December 2021).
41. Butorov, V.P.; Nichkov, I.F.; Novikov, E.A.; Raspopin, S.P. Izv. Vyssh. Ucheb. Zaved. Tsvetn. Met. 1973, 15, 96.
42. Hoshino, Y.; Plambeck, J.A. Electrochemical studies of yttrium and ytterium-zinc alloys in fused LiCl-KCl eutectic. Can. J. Chem. 1970, 48, 685–687.
43. Yamschikov, L.F.; Lebedev, V.A.; Nichkov, N.F. Metally. Izv. Akad. Nauk SSSR 1979, 83.
44. Marquina, C.; Kim-Ngan, N.H.; Bakker, K.; Radwanski, R.J.; Jacobs, T.H.; Buschow, K.H.J.; Franse, J.J.M.; Ibarra, M.R. Specific heats of R2Zn17 intermetallic compounds. J. Phys. Condens. Matter. 1993, 5, 2009.
45. Morishita, M.; Yamamoto, H.; Tsuboki, K.; Horike, T. Standard Gibbs energy of formation of Zn17Y2 and Zn12Y determined by solution calorimetry and measurement of heat capacity near zero kelvin. Int. J. Mater. Res. 2007, 98, 10–15.
46. Zhu, Z.; Pelton, A.D. Critical assessment and optimization of phase diagrams and thermodynamic properties of RE–Zn systems—Part II—Y–Zn, Eu–Zn, Gd–Zn, Tb–Zn, Dy–Zn, Ho–Zn, Er–Zn, Tm–Zn, Yb–Zn and Lu–Zn. J. Alloys Compd. 2015, 641, 261–271.
47. Ghosh, P.; Mezbahul-Islam, M.; Medraj, M. Critical assessment and thermodynamic modeling of Mg-Zn, Mg-Sn, Sn-Zn and Mg-Sn-Zn systems. Calphad 2012, 36, 28–43.
48. Islam, M.M.; Kevorkov, D.; Medraj, M. The equilibrium phase diagram of the magnesium-copper-yttrium system. J. Chem. Thermodyn. 2008, 40, 1064–1076.
49. Gröbner, J.; Kozlov, A.; Fang, X.Y.; Geng, J.; Nie, J.F.; Schmid-Fetzer, R. Phase equilibria and transformations in ternary Mg-rich Mg-Y-Zn alloys. Acta Mater. 2012, 60, 5948–5962.
50. Zhu, Z.; Pelton, A.D. Thermodynamic modeling of the Y-Mg-Zn, Gd-Mg-Zn, Tb-Mg-Zn, Dy-Mg-Zn, Ho-Mg-Zn, Er-Mg-Zn, Tm-Mg-Zn and Lu-Mg-Zn systems. J. Alloys Compd. 2015, 652, 426–443.
51. Le, Q.C.; Zhang, Z.Q.; Shao, Z.W.; Cui, J.Z.; Xie, Y. Microstructures and mechanical properties of Mg-2%Zn-0.4%Re alloys. Trans. Nonferr. Met. Soc. China 2010, 20, 352–356.
52. Singh, A.; Somekawa, H.; Mukai, T. High temperature processing of Mg–Zn–Y alloys containing quasicrystal phase for high strength. Mater. Sci. Eng. A 2011, 528, 6647–6651.
53. Liu, P.; Jiang, H.; Cai, Z.; Kang, Q.; Zhang, Y. The effect of Y, Ce and Gd on texture, recrystallization and mechanical property of Mg-Zn alloys. J. Magnes. 2016, 4, 188–196.
54. Singh, A. Tailoring microstructure of Mg-Zn-Y alloys with quasicrystal and related phases for high mechanical strength. Sci. Technol. Adv. Mater. 2014, 15, 44803.
55. Jian, W.W.; Cheng, G.M.; Xu, W.Z.; Koch, C.C.; Wang, Q.D.; Zhu, Y.T.; Mathaudhu, S.N. Physics and model of strengthening by parallel stacking faults. Appl. Phys. Lett. 2013, 103, 133108.
56. Du, Y.; Zheng, M.; Qiao, X.; Jiang, B. Enhancing the strength and ductility in Mg-Zn-Ce alloy through achieving high density precipitates and texture weakening. Adv. Eng. Mater. 2017, 19, 1700487.

Retrieved from https://encyclopedia.pub/entry/history/show/41909